MASS TRANSFER DEPOSITS IN LITHIUM-TYPE 316 STAINLESS STEEL THERMAL-CONVECTION LOOPS*

P. F. Tortorelli, J. H. DeVan

Metals and Ceramics Division
Oak Ridge National Laboratory
Oak Ridge, Tennessee 37830

MASTER

CONF-800401--6

ABSTRACT

In spatially nonisothermal flowing liquid metal systems, selected constitutents of the containment material characteristically dissolve into the liquid metal in the hotter zones and are deposited in the colder areas. The accumulation of deposits is often a more serious problem than dissolution because of attendant flow restrictions and, in reactor applications, the aggregation of radioactive species in the coolant circuits. Accordingly, we studied the deposition processes in lithium-type 316 stainless steel thermal convection loops. The morphology and composition of deposits varied with loop operating time. Initially, chromium-rich dendritic crystals formed in the colder region of a loop, but later the deposits changed in structure and contained significant amounts of nickel and iron. Deposition rates were also measured as a function of time and temperature and were correlated with the above observations. A plug extracted from one loop consisted of an aggregate of chromium-rich crystals.

INTRODUCTION

The possible uses of lithium as a coolant and/or tritium-breeding fluid in fusion reactors have renewed interest in the compatibility of molten lithium with structural materials. Compatibility

*Research sponsored by the Office of Fusion Energy, U.S. Department of Energy, under contract W-7405-eng-26 with the Union Carbide Corporation.

problems include the loss of material by corrosion as well as the development of flow restrictions and accumulations of radioactive species by mass transfer of the dissolved elements to the cooler parts of lithium circuits. The present study was conducted to determine the time dependence of the deposition phenomena and the characteristics of mass transfer deposits in type 316 stainless steel lithium thermal-convection loops. The time dependence of the dissolution process in this system was discussed earlier.[1]

EXPERIMENTAL PROCEDURES

The Li used in this study was purified by cold-trapping[2] and subsequent heating at 815°C for 100 h in a Ti-lined pot containing Zr foil. Typical impurity concentrations of the pruified Li were 30 to 100 wt ppm N and 30 to 130 wt ppm O. This Li was then used to fill three type 316 stainless steel loops (see Fig. 1) that contained corrosion coupons (19.1 by 7.9 by 0.9 mm) of the same steel composition. The loop arrangement allowed the coupons to be retrieved and returned to the heated (hot) and cooled (cold) legs without stopping the Li flow. As shown in Fig. 1, the coupons were labeled according to their positions in the hot (H) or cold (C) legs. They were weighed before loop operation and at intervals during the experiment to establish weight

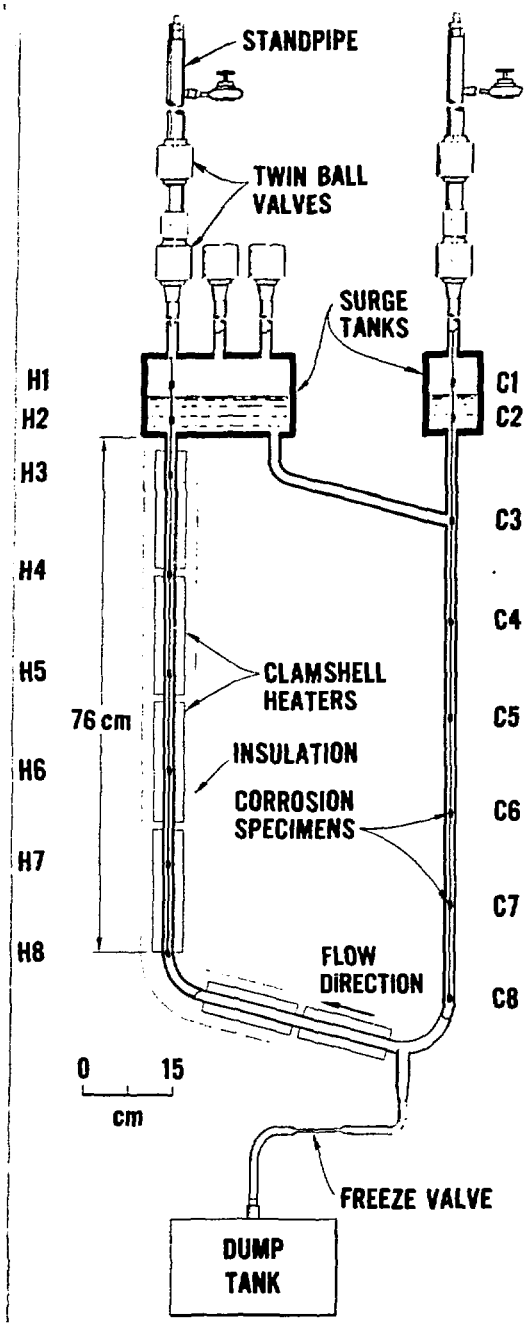

FIGURE 1. Thermal Convection Loop with Accessible Corrosion Coupons.

change profiles as a function of time. Small quantities of the circulating lithium were periodically removed from the loop to measure impurity concentrations. During the present experiments the concentrations in Li ranged from 30 to 130 wt ppm N and 85 to 135 wt ppm O. The natural circulation

of Li was maintained by establishing a fixed thermal gradient around the loop. The maximum Li temperature was held at 600°C at the top of the hot leg (just above H3), while the flow rate was adjusted by means of a tapered valve at the bottom of the hot-leg surge tank so that the lowest Li temperature was about 450°C (near C8). The flow velocity in these loops for this ΔT of 150°C was approximately 30 mm/s and was determined by heating a small spot on a loop wall for a few seconds and measuring the time for the heat pulse to cause a temperature rise at a thermocouple located at a known distance downstream. Velocities measured by this method were in reasonable accord with those obtained from heat transfer calculations.[3]

(cap delta)

In addition to the weight changes, the mass transfer process was studied by use of optical and scanning electron microscopy. Compositions of the near-surface regions of the insert coupons and corrosion deposits were determined by x-ray fluorescence, electron microprobe analysis, and/or x-ray diffraction.

The operations of loops 1 and 2 had to be terminated because of flow restrictions after 9000 and 4000 h, respectively. Both cold legs were replaced and the loops were put back into operation with new specimens.

RESULTS

The coupons from the three loops were weighed after intervals of at least 500 h. Any one particular weighing resulted in a mass transfer profile such as the one shown in Fig. 2, while a series of weighings yielded data on the coupon weight losses and gains as a function of exposure time. Weight gain versus time plots for loops 1, 2, and 3 for the coupons in the C8 position

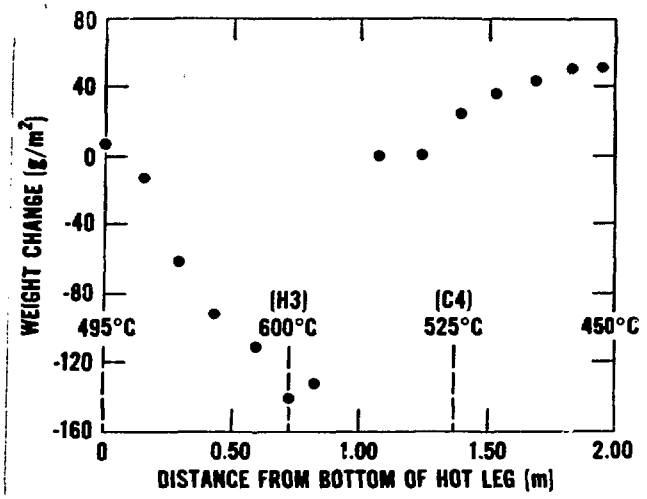

FIGURE 2. Weight Change vs Coupon Position in a Loop Operated for 9000 h. Distance is measured in direction of flow.

(about 460°C, see Fig. 1) are given in Fig. 3. The two sets of data for loop 2 represent operation (A) before and (B) after replacing part of its cold leg. The deposition rate for a particular location was determined from the least squares slope of the plot of weight gain against exposure time for the specimen at that position. The resultant deposition rates are given in Table I. Note that the rates computed for the longer test times (>3700 h) are significantly less than those from shorter exposure measurements. This decrease in deposition rate with time is also apparent in Fig. 3(b). The data in Table I also show that the maximum deposition rate occurred near the middle of the cooled region of a loop.

The morphology and composition of the depositions on the coupons in the cold legs varied with time. After relatively short exposures (<2000 h), Cr-rich dendritic crystals were observed on cold-leg coupons. Examples of these crystals are shown by the scanning electron micrographs in Fig. 4. Energy-dispersive x-ray analysis indicated

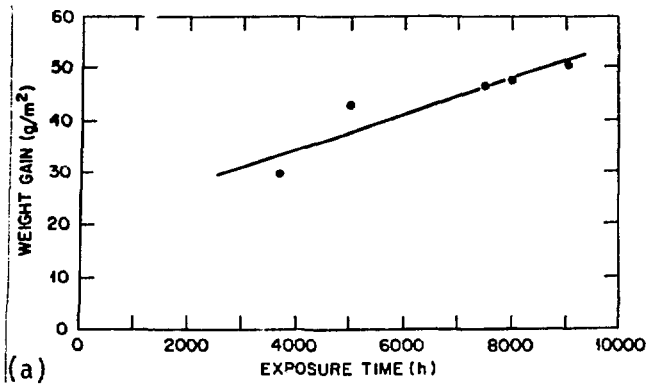

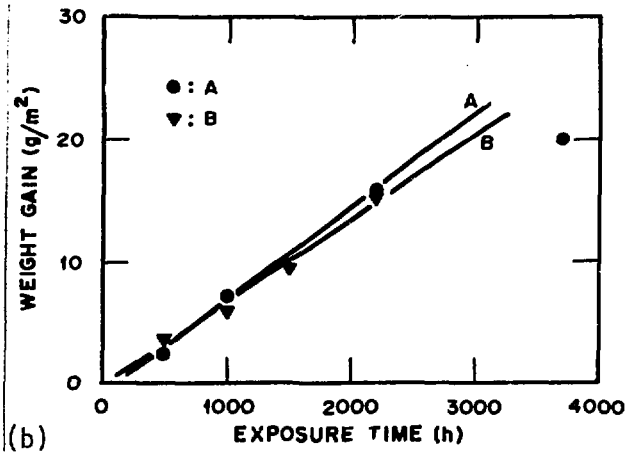

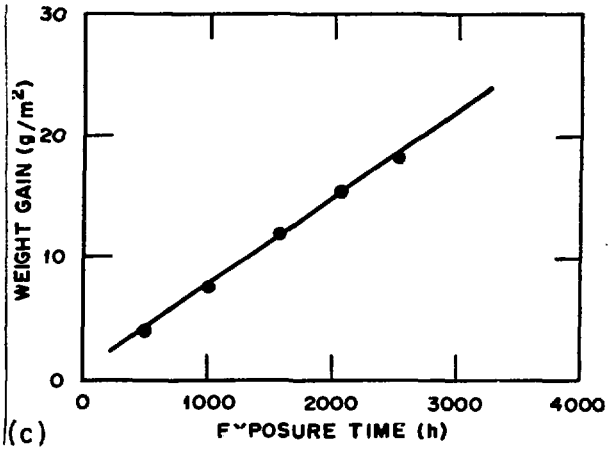

FIGURE 3. Weight Gain vs Time at 460°C. (a) Loop 1. (b) Loop 2. A: Coupon in original loop. B: Coupon after replacement of cold leg. (c) Loop 3.

that the approximate composition of the crystals was 95% Cr, 4% Fe, 1% Ni. At longer operating times the deposits tended to be less needle-like and were more contiguous, appearing as a highly faceted

TABLE I. DEPOSITION RATES FOR LITHIUM-TYPE 316 STAINLESS STEEL THERMAL-CONVECTION LOOPS

Coupon	Temp (°C)	Deposition Rate,(a) mg/m^2 h			
		Loop 1	Loop 2		Loop 3
			A	B	
C4	525	1.3	7.2	5.6	7.5
C5	510	2.8	7.0	8.1	8.6
C6	490	3.2	7.6	8.2	8.0
C7	475	4.2	7.4	7.2	8.1
C8	460	3.3	7.8	7.0	7.2

(a)Operating intervals for each loop: 1, 3750–9034 h; 2, <2200 h; 3 <2520 h.

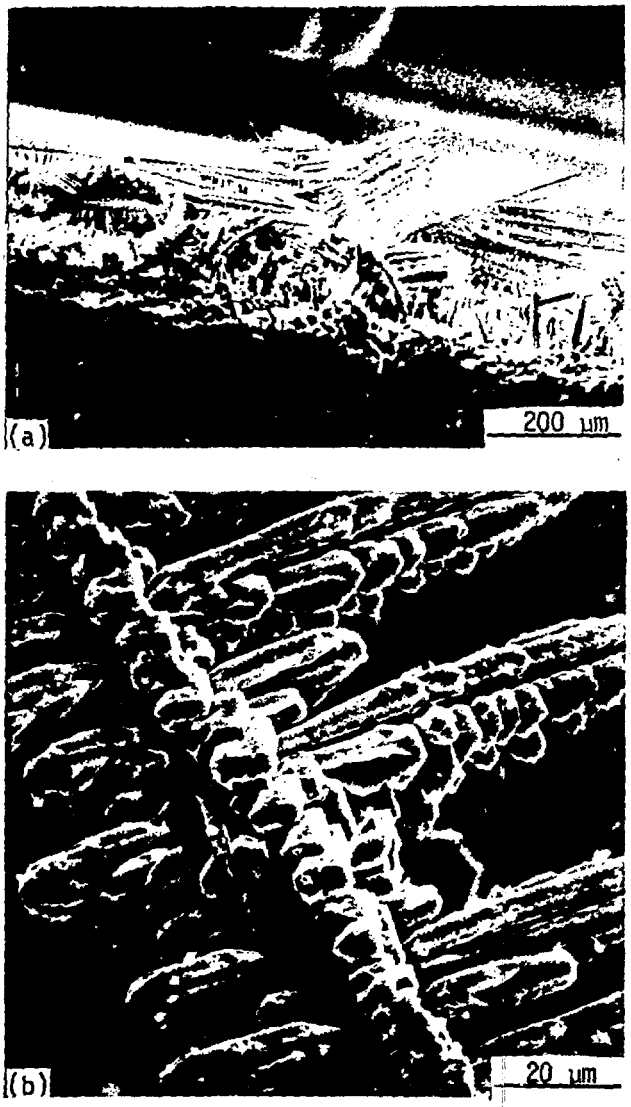

FIGURE 4. Chromium Crystals That Formed in the Cold Leg of a Type 316 Stainless Steel-Lithium Loop After 1700 h at 460°C. (a) Cross section. (b) Top view.

surface layer on cold leg coupons (see Fig. 5). The compositions of the latter deposits depended on the distance above the original coupon surface. The underlying, or earlier, deposits (such as B Fig. 5) were principally Cr, while the top (later) ones (A) contained significant amounts of Fe, Ni, and Cr. This gradient in deposit composition is clearly shown in Fig. 6, which is an optical micrograph of a coupon cross section with corresponding spectra from electron microprobe analysis. Similar deposits were observed on coupons at various positions in the cold leg.

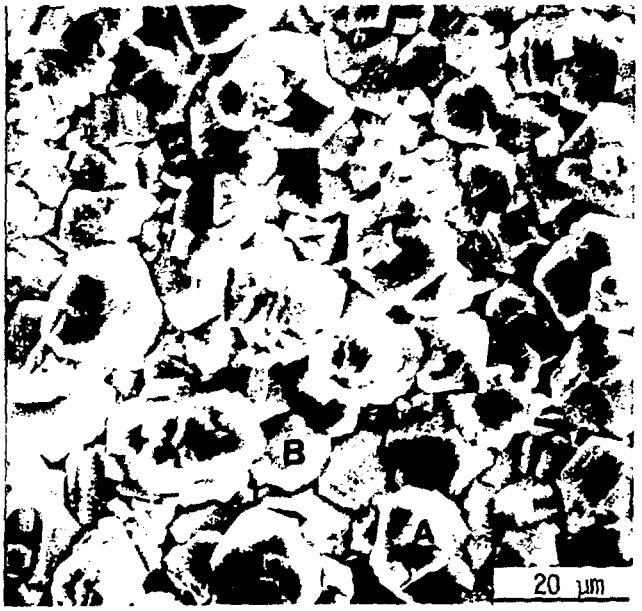

FIGURE 5. Deposits on a Coupon in a Lithium Type 316 Stainless Steel Thermal-Convection Loop Exposed at 460°C for 9000 h. A: Cr-Fe-Ni deposit. B: Cr-rich deposit.

As mentioned above, cold-leg deposits in loops 1 and 2 eventually blocked the flow. The lower bend in the cold leg of loop 1 (see Fig. 1) was cut out and split longitudinally, and a plug was found near the coldest point of the circuit. This location was below the zone of the cold leg in which we were able to locate removable

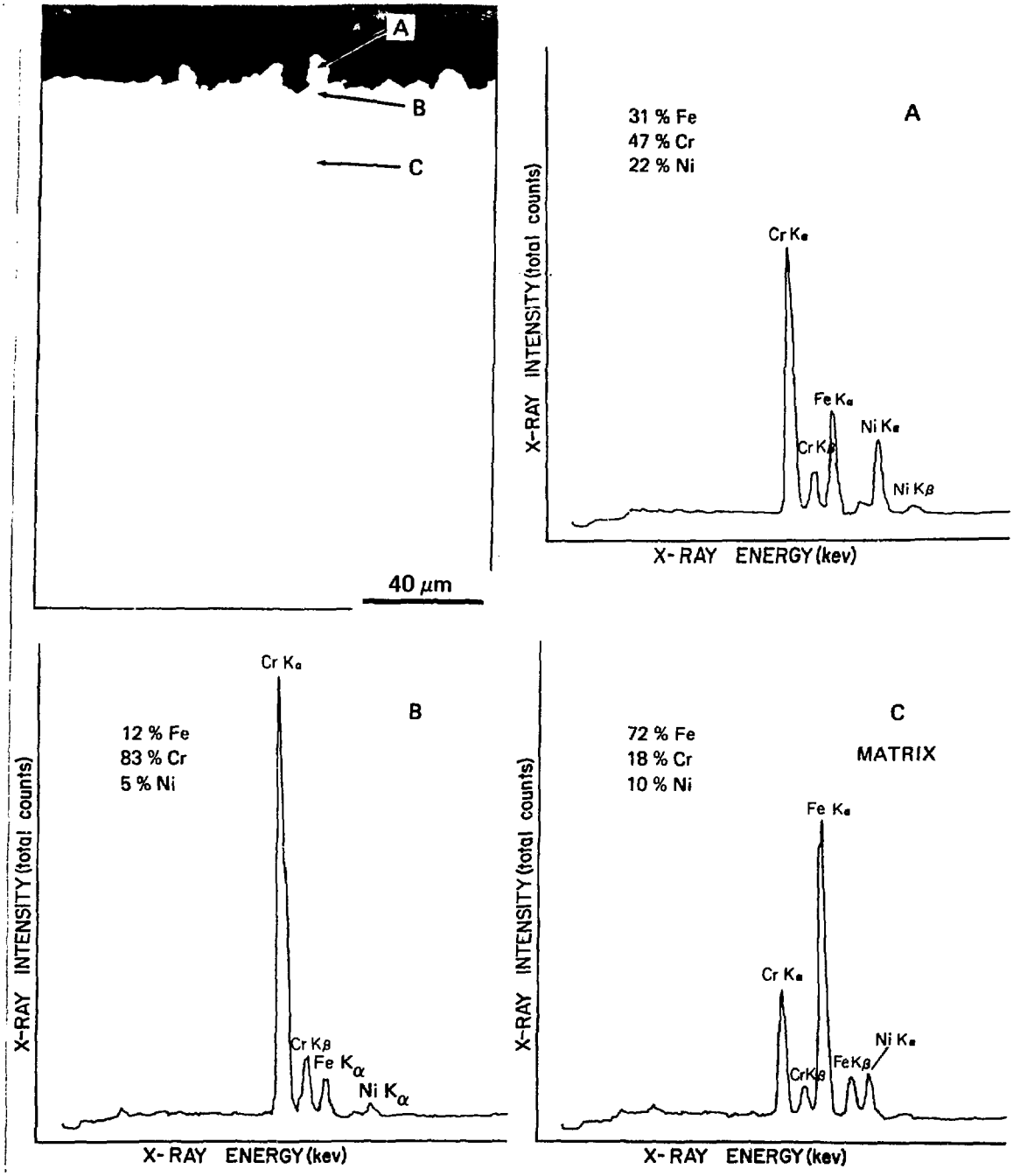

FIGURE 6. Electron-Beam Microanalysis of the Deposits on a Coupon in a Lithium-Type 316 Stainless Steel Thermal-Convection Loop at 460°C after 9000 h.

specimens. This procedure was repeated for loop 2, and the vestiges of a similar plug were apparent, although in this case most of the plug had apparently been dislodged when the Li was drained before the cold leg section was removed. At room temperature the plug in loop 1 consisted of a mass of Li with imbedded metallic crystals. Examination of a piece of the plug in a scanning electron microscope revealed the crystals to be mainly Cr-rich dendrites (see Fig. 7), which were concentrated toward the downstream side of the plug. Some Ni-rich crystals were also found.

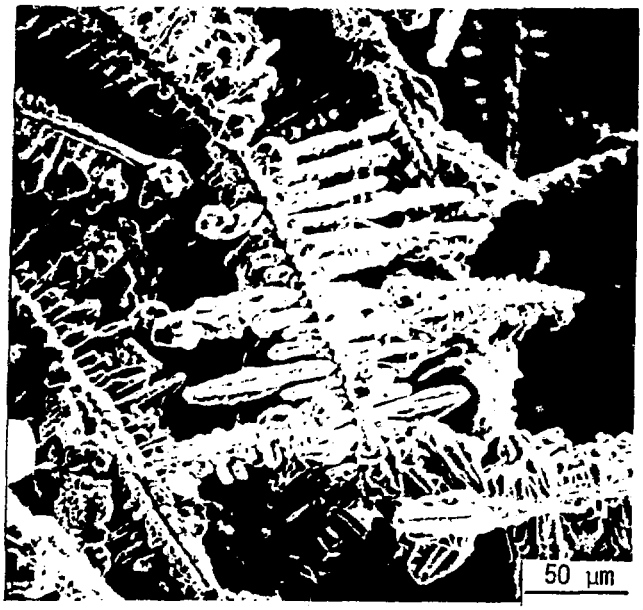

FIGURE 7. Chromium Crystals Found in a Mass Transfer Plug from a Lithium Type 316 Stainless Steel Loop that Operated for 10,000 h.

DISCUSSION

As shown in Fig. 2, the dissolution of the stainless steel in the hot zone of these loops was accompanied by the deposition of material in the cooler regions. Studies[4,5] of dissolving specimens indicated that dissolution begins with the preferential leaching of Ni and Cr and ultimately reaches a steady-state regime where each element of the stainless steel dissolves in proportion to its bulk concentration. Weight loss plotted against exposure time reflects this behavior;[1] initial corrosion rates are high and correspond to the preferential removal of Ni and Cr from the steel. At longer times the rates decrease and become constant with time as a steady state is attained.

The time dependence of weight gain at position C8 in the three loops is shown in Table I and Fig. 3. Note that the gain in weight at this position is linear with time up to between 3000 and 4000 h; then the

rate of gain markedly decreases. Along with the varying dissolution and deposition rates, the deposit morphology and composition also changed with loop operating time (for example, see Fig. 6). When Cr and Ni were preferentially leached in the hot zone during the first few thousand hours of loop operation, Cr was deposited at position C8 in the form of highly branched, needle-like dendrites. At longer exposures, when Fe, Ni, and Cr were being released into the Li in the same proportions as their bulk concentration, the deposits at C8 were more contiguous and contained Fe and Ni in addition to Cr. Kolster and Bos[6] have observed a similar two-stage process for type 316 stainless steel in sodium with less than 8 ppm O. They found Cr-rich carbide layers in the cooled regions. Above these layers were metallic deposits similar in composition to austenitic stainless steel.

A companion paper[4] treats the kinetics of the mass transfer process in lithium-stainless steel loops in terms of the rate equation

$$R = k(i)[C_s(i) - C_x(i)] \ , \qquad (1)$$

where

R = the rate of dissolution (+) or deposition (−),

$k(i)$ = the rate constant for the dissolution (k_s) or deposition (k_p) of element i,

$C_s(i)$ = the solubility of i in Li at temperature T, and

$C_x(i)$ = the actual concentration of i in Li at point x in the loop; it eventually becomes constant with time.

When C_x is greater than C_s deposition occurs. Although relatively large amounts of both Cr and Ni were dissolved into the Li during the first few thousand hours of loop operation, the loop areas accessible to removable specimens in this study showed mainly Cr deposition. One explanation for this observation, which we discount, assumes that the constant C_x value for Cr was attained much more rapidly than C_x for Ni, and therefore Cr deposited sooner. This is the equivalent of stating that the dissolution rate constant (k_s) of Cr is greater than that of Ni. However, given the solubilities of Cr and Ni in Li and the relative rates of dissolution of Cr and Ni, the times required to reach solute concentrations near C_x are extremely short compared with even the first sampling time.

A more credible possibility is that at early operating times, when enhanced leaching of Cr is occurring in the hot leg, the activity of Cr in the Li is sufficiently large to cause pure Cr precipitation in the cold leg. After nucleation of these crystals the dendritic growth of these deposits increased the available surface area for deposition. This increase in surface area may have just offset the decreasing Cr activity in the Li to produce the observed linear deposition rate between 3000 and 4000 h. Eventually, the surface area reached a constant value and, combined with the decreased Cr activity, led to the significantly lower deposition rate at longer times. This explanation, however, does not account for the absence of Ni deposition during initial loop operation. It is difficult to speculate on the reason for this because of a lack of detailed analytical data on the surface compositions

of cold leg coupons after short exposures. This situation stemmed from the need to follow the weight changes of the coupons out to extended operating times and thus precluded destructive examination of the insert specimens.

Another factor that needs to be considered in trying to explain the formation of pure Cr crystals is the role that impurities in the Li may play in the deposition process. For example C and/or N could be intermediates in the formation of Cr crystals. Kolster and Bos[6] observed Cr-rich carbide layers as the initial deposition product in the cooled regions of type 316 stainless steel circuits of low-oxygen sodium, and Hoffman[7] has found Cr carbide deposits in lithium-stainless steel thermal-convection loops. In contrast, x-ray diffraction of the Cr dendrites found in the mass-transfer plug showed them to have the lattice parameter of pure Cr. Nevertheless, impurities may have affected the deposition process by forming precursor Cr carbides or nitrides that then decomposed as the local activities changed. It is interesting that the precipitation of Cr dendrites from a Li bath has been observed during experiments[8] to measure the solubility of Cr in Li, but the possible effect of impurities on the process is unknown.

As seen from Table I, the maximum deposition rates occurred in the central part of the cold leg. This behavior can be attributed to a competition between two factors.[9] As seen in Eq. (1), the deposition rate is a product of the rate constant (k) and the supersaturation. Since the former decreases while the latter increases with decreasing temperature, the maximum

deposition rate should occur at an intermediate temperature (which happens to be near the middle of the cold leg).

The plugging that ultimately occurred in these lithium-type 316 stainless steel thermal-convection loops poses a serious problem for Li systems using austenitic stainless steels by not only restricting flow but by causing the accumulation of radioactive elements. The problem is exacerbated by the geometry of dendrites, which can bridge to form massive tangles. The positional dependence of Cr deposition in these loops suggests that the plug of Cr crystals was not formed by deposition in situ but occurred because of the settling or trapping of Cr dendrites at the bend, which was the gravitationally lowest point in our loop. Hoffman[7] has reported similar tangles of mass transfer crystals at the same point in type 316 stainless steel-lithium thermal-convection loops of slightly different design.

Following the replacement of the plugged regions in loops 1 and 2 no change in the flow characteristics of these loops could be detected in 4000 h of additional operation. We assume that the deposits now being formed are of a morphology and composition similar to those shown in Fig. 5 and that plugging caused by Cr dendrites should be a transient effect associated with initial loop operation. Confirmation of this point would mean that a Li system could conceivably be designed to accommodate or trap these high-aspect-ratio crystals during early operation and that deposition rates thereafter would be acceptable in terms of longer term flow restictions.

SUMMARY

The local weight gains for insert specimens in flowing lithium-type 316 stainless steel systems were linear with time, but the deposition rate decreased sharply after between 3000 and 4000 h. The deposit morphology and composition also changed with loop operating time. Initially, Cr-rich dendritic deposits were formed in the cooled loop regions; later the deposit composition changed toward greater concentrations of Fe and Ni.

Chromium dendrites led to severe flow restrictions in two thermal-convection loops. After replacement of the plugged regions in these loops, operation continued for 4000 h without any further flow restrictions. Hence, we believe that these Cr-rich deposits are only an initial transient effect, and it may be possible to design around this plugging problem in lithium-stainless steel systems.

ACKNOWLEDGEMENTS

The authors acknowledge the contribution of E. J. Lawrence, who was responsible for the design and operation of the thermal-convection loops used in this study. We thank R. S. Crouse for the electron microprobe analysis and scanning electron microscopy and O. B. Cavin for the x-ray diffraction results. Thanks are also due to C. J. Long, Jr., and C. T. Liu for their reviews of the manuscript, S. Peterson for the editing, and S. G. Frykman for report preparation.

REFERENCES

1. P. F. Tortorelli and J. H. DeVan, "Thermal-Gradient Mass Transfer in Lithium-Stainless Steel Systems," *J. Nucl. Mater.* 85 and 86, 289–93, 1979.

2. H. Bradley et al., *Purification of Lithium by Cold Trapping*, GESP-593, General Electric, November 1971.

3. P. F. Tortorelli, J. H. DeVan, and J. E. Selle, *Corrosion of Austenitic Stainless Steels in Flowing Lithium*, Oak Ridge National Laboratory report in preparation.

4. P. F. Tortorelli, J. H. DeVan, and J. E. Selle, "Corrosion in Lithium/Stainless Steel Thermal-Convection Systems," *Proc. Second Int. Conf. on Liquid Metal Technology in Energy Production*, American Nuclear Society, Richland, Washington, April 21–24, 1980.

5. E. G. Brush, *Sodium Mass Transfer. XVI. The Selective Corrosion Component of Steel Exposed to Flowing Sodium*, GEAP-4832, General Electric, March 1965.

6. B. H. Kolster and L. Bos, "Corrosion, Transport, and Deposition of Stainless Steel in Liquid Sodium," pp. 368–77 in *Proc. Int. Conf. Liquid Metal Technology in Energy Production*, CONF-760503-P1, May 1976.

7. E. E. Hoffman, *Corrosion of Materials by Lithium at Elevated Temperatures*, ORNL-6274, Oak Ridge National Laboratory, March 1959.

8. N. M. Beskororainyi and E. I. Yakovlev, *Met. Metalloved. Chistykh Metal., Sb. Nauchn. Rabot* 2: 189–206 (1960) as cited by R. P. Elliott, *Constitution of Binary Alloys, 1st Supplement*, McGraw-Hill, New York, 1965, p. 350.

9. J. H. DeVan, "Corrosion of Iron- and Nickel-Base Alloys in High-Temperature Sodium and NaK," pp. 643–59 in *Alkali Metal Coolants*, International Atomic Energy Authority, Vienna, 1967.